Carbohydrate Polymers 89 (2012) 98–103

Contents lists available at SciVerse ScienceDirect

Carbohydrate Polymers

journal homepage: www.elsevier.com/locate/carbpol

# On the interaction between konjac glucomannan and xanthan in mixed gels: An analysis based on the cascade model

Ching-Feng Mao*, Worasaung Klinthong, Yuan-Chang Zeng, Cheng-Ho Chen

*Department of Chemical and Materials Engineering, Southern Taiwan University, No. 1, Nan-Tai St., Yongkang Dist., Tainan City 710, Taiwan, ROC*

ARTICLE INFO

*Article history:*
Received 4 July 2011
Received in revised form 24 August 2011
Accepted 21 February 2012
Available online 5 March 2012

*Keywords:*
Konjac glucomannan
Xanthan
Mixed gels
Cascade model

ABSTRACT

The rheological properties and critical behavior of konjac glucomannan (KGM)/xanthan (XG) mixed gels were investigated and analyzed using a two-component cascade model. The fitting results show that the optimal functionality value for KGM ($f_{KGM}$) is 3, whereas the possible functionality value for XG ($f_{XG}$) is 100–1000 obtained from the modulus data, or 25 obtained from the critical data. The van't Hoff analysis of the critical data shows that the binding of KGM with XG has a high enthalpy/entropy ratio ($\Delta H/300\Delta S = 5.52$), which can be explained by the gain in the hydrational entropy due to the release of water molecules during the binding reaction. From these results, we proposed that the binding of KGM with XG takes place on the consecutive glucose residues of KGM with six or more units.



## 1. Introduction

The synergistic interaction between xanthan gum (XG) and konjac glucomannan (KGM) has attracted the attention of many researchers because of its unusual gelling properties and potential applications. On its own, the XG solution exhibits a weak gel behavior at moderate concentrations (Ross-Murphy, Morris, & Morris, 1983), while an irreversible gelation of the KGM solution can be induced by adding an alkaline coagulant (Maekaji, 1974). When mixing KGM and XG in comparable amounts, a strong thermo-reversible gel can be formed (Dea et al., 1977). Due to the enhanced strength and easy processing, the mixed gel finds applications in food science (Agoub, Smith, Giannouli, Richardson, & Morris, 2007) and drug delivery systems (Alvarez-Mancenido, Lacik, Landín, & Martínez-Pacheco, 2008).

Xanthan gum is a natural polysaccharide consisting of a β-1,4-linked D-glucose backbone, substituted alternately with a trisaccharide side chain linked to every second glucose residue (Jansson, Kenne, & Lindberg, 1975; Melton, Mindt, Rees, & Sanderson, 1976). The side chain consists of a glucuronic acid residue between two mannose residues, which are partially acetylated and may contain pyruvic acid. Xanthan in aqueous solutions maintains a rigid structure with ordered conformation as a double-stranded helix with a persistence length of approximately 150 nm (Berth et al., 1996). Under heat treatment, it undergoes an order-disorder transition from helix to random coil (Milas & Rinaudo, 1979, 1986). The transition temperature can be altered by factors such as pH (Agoub et al., 2007), ionic strength (Milas & Rinaudo, 1979), and content of pyruvate and acetate substituents (Smith, Symes, Lawson, & Morris, 1981). A weak XG gel can be formed due to the association of XG helices above a critical concentration (Rodd, Dunstan, & Boger, 2000).

Konjac glucomannan is a neutral polysaccharide consisting of β-1,4-linked D-mannose and D-glucose units with a mannose/glucose ratio of around 1.6 (Katsuraya et al., 2003; Maeda, Shimahara, & Sugiyama, 1980). An acetyl group is attached to the KGM backbone (approximately one per 19 residues), which confers its solubility in water (Maeda et al., 1980; Maekaji, 1974). In the absence of acetyl groups, the glucomannan is insoluble in water. The deacetylation reaction can be induced by reacting KGM with alkali upon heating. This process results in a thermally irreversible KGM gel, where its junction zone is formed via the aggregation of deacetylated KGM segments (Maekaji, 1974).

When mixing KGM with XG, a thermo-reversible gel can be produced with a gel strength comparable to that of mixed galactomannan/xanthan gels (Goycoolea, Richardson, Morris, & Gidley, 1995). The synergistic interaction has been proposed to occur by the attachment of segments of galactomannan or glucomannan to the cellulose backbone of disordered xanthan segments, rather than to the xanthan helix (Brownsey, Cairns, Miles, & Morris, 1988; Cairns, Miles, & Morris, 1986; Cairns, Miles, Morris, & Brownsey, 1987). This hypothesis is supported by two facts: (i) the appearance of new X-ray fiber patterns assigned to the binding between xanthan and galactomannan for oriented mixed gels, and (ii) the suppression of gelation for mixing under conditions where xanthan is in the helix conformation. The interacting site of galactomannans was

* Corresponding author. Tel.: +886 6 2533131x3728; fax: +886 6 2425741.
*E-mail address:* cfmao@mail.stut.edu.tw (C.-F. Mao).

0144-8617/$ – see front matter © 2012 Elsevier Ltd. All rights reserved.
doi:10.1016/j.carbpol.2012.02.056

suggested to be composed of consecutive unsubstituted mannan segments (Dea, Clark, & McCleary, 1986), which was confirmed by the observation of the synergistic gelation of galactose-depleted guar gum and xanthan (McCleary, Amado, Waibel, & Neukom, 1981; Pai & Khan, 2002). However, little was known about the binding site of KGM in mixed gels. A comparison of the X-ray fiber patterns of oriented mixed gels for the galactomannan/xanthan and the glucomannan/xanthan systems showed that the structure of their binding site is different (Brownsey et al., 1988). Substantial differences were also observed in the thermogram and the variation of rheological properties during a cooling process (Goycoolea et al., 1995). A possible model is that the binding site in KGM/XG mixed gels involves the segment of glucose residues of KGM, rather than the segment of mannose residues.

In our previous work we have shown that the synergistic gelation of unlike polysaccharides can be modeled by a two-component cascade model (Mao, 2006; Mao & Chen, 2006). This model was applied to analyze the concentration dependence of gel modulus or critical gelling data for mixed galactomannan/xanthan gels (Mao & Rwei, 2006). The analysis results provided information about the number of cross-linking segments for a galactomannan or xanthan molecule and the enthalpy change for the cross-linking reaction, which were helpful in understanding the interacting site of mixed gels. In this work, the gelling properties of KGM/XG mixtures were investigated and analyzed based on the two-component cascade model. The fitted model parameters were correlated with the chemical structure of the component polysaccharides, and an attempt was made to justify the hypothesis that the binding site of the mixed gel involves the segment of glucose residues of KGM.

## 2. Materials and methods

### 2.1. Materials and sample preparation

Xanthan and konjac glucomannan were purchased from Aldrich (Milwaukee, WI) and Shimizu Chemical (Hiroshima, Japan), respectively. The intrinsic viscosities obtained from an Ubbelohde capillary viscometer for XG in 0.10 M NaCl and KGM are 15.8 and 14.2 dl/g, respectively. The average molecular weights are estimated to be $9.80 \times 10^5$ and $4.75 \times 10^5$ g/mol for XG and KGM, respectively, using the Mark–Houwink equation (Capron, Brigand, & Muller, 1997; Prawitwong, Takigami, & Phillips, 2007).

KGM/XG mixed gels were prepared by dispersing appropriate amounts of KGM and XG in de-ionized water to give a desired concentration ratio ($r = C_{KGM}/C_{XG}$) by stirring at room temperature for 30 min. Sodium azide of 0.05 wt% was added to prevent bacterial degradation. The samples were then heated at 80 °C for 1 h. Gelation was observed when the samples were cooled to room temperature.

### 2.2. Rheological measurements

Rheological measurements were performed using a controlled stress rheometer (Physica MCR 501, Anton Paar Germany GmbH). The hot solution was poured into the rheometer measuring system (parallel plate geometry, 25 mm diameter, and 0.5 mm gap) and allowed to cool to room temperature. Measurements were carried out after the sample temperature has stabilized at 25 °C for 10 min. A strain sweep test was performed to check that measurements have been performed within the linear viscoelastic (LVE) regime. The shear storage modulus ($G'$) at 25 °C was recorded for samples at different polysaccharide concentrations and KGM/XG concentration ratios.

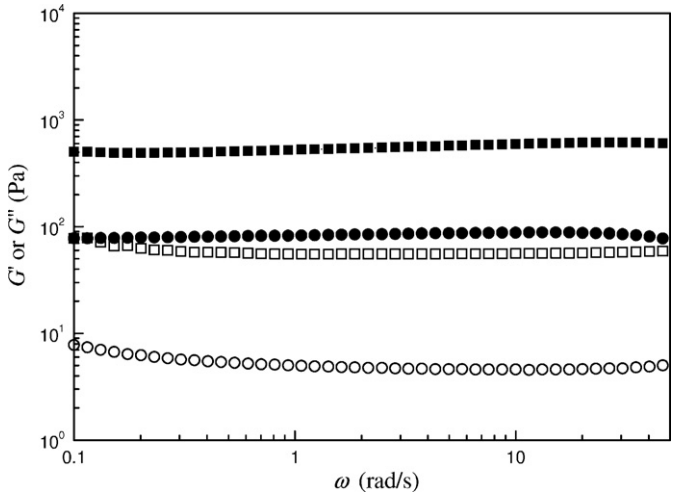


**Fig. 1.** Frequency sweep of KGM/XG solutions ($C_{KGM}/C_{XG} = 1$) at 25 °C (filled and open symbols represent $G'$ and $G''$, respectively; (●/○) $C = 5$ g/L; (■/□) $C = 15$ g/L.

### 2.3. Determination of critical concentrations

The melting temperature of the KGM/XG gels was determined by the "test tube upside-down" method (Hong & Chen, 1998). The sample was sealed in a test tube of 10 mm id, which was immersed in a water bath, and the temperature was allowed to rise at a rate of 1 K/min approximately. The temperature at which the gel started to flow was recorded as the gel melting temperature. The thermo-reversibility characteristic of the mixed gel can be readily demonstrated in repeated runs of the same sample, where an identical melting temperature was obtained. The concentration dependence of the melting temperature was analyzed using the Ferry–Eldridge equation (Eldridge & Ferry, 1954). The critical concentration at a specific temperature was obtained from the interpolation of the Ferry–Eldridge plot.

## 3. Results and discussion

### 3.1. Rheological properties and modulus–composition relations

Pure xanthan or konjac glucomannan solutions exhibit fluid-like rheological behavior, while a strong gel can be produced by mixing these two fluids. Fig. 1 shows the typical frequency sweeps of the KGM/XG solutions with a concentration ratio of $r = 1$ at room temperature. It is evident that the storage modulus $G'$ is one order of magnitude larger than the loss modulus $G''$ and both moduli are frequency-independent, corresponding to a strong gel behavior. The value of the storage modulus varies as a function of both polysaccharide concentration and concentration ratio, which characterizes the number density of interacting sites of a mixed gel.

The synergistic effect of a mixed polysaccharide system can be elucidated by examining the property change with respect to the composition. Experimental results for composition dependence of the storage modulus at a fixed polysaccharide concentration are presented in Fig. 2. It can be seen that the storage modulus reaches a maximum at $r = 2$ with a value much greater than those of the individual components, indicating the existence of a strong synergism between KGM and XG. The asymmetry of the composition dependence curve in Fig. 2 implies that the number of interacting sites in a polysaccharide chain (functionality) for KGM and XG are quite different. In the later analysis we will show that the functionality of KGM is much less than that of XG.

A second series of experiments was carried out in order to study the polysaccharide concentration dependence of storage modulus

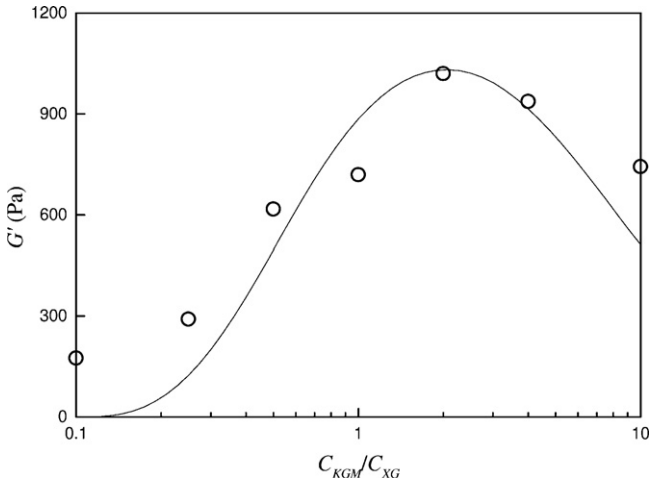


**Fig. 2.** Composition dependence of the storage modulus for KGM/XG gels ($C$ = 20 g/L) at 25 °C. The curve is derived by the cascade model using the parameters at the functionality set ($f_{KGM}$, $f_{XG}$) = (3, 100).

at different mixing ratios. The moduli for samples of $r$ = 2 are consistently higher than those of different mixing ratios at all concentrations, as shown in Fig. 3. The concentration dependence of storage modulus for physical gels can be simply approximated by a power law, $G' \propto C^n$, where $n$ is an empirical exponent. The parameter $n$ is found to be close to 2.2 at $r$ = 0.5 and decreases with increasing mixing ratio ($n$ = 1.7 and 1.5 for $r$ = 1 and 2, respectively). It has been reported that an $n$ value of 2.25 corresponds to physical gels with an extremely high functionality, while a lower $n$ value indicates the existence of a low functionality (Clark & Ross-Murphy, 1985). Thus, the decrease in $n$ values with increasing KGM content suggests that the functionality of KGM is lower than that of XG. In order to obtain the exact $f$ values for KGM and XG, the experimental data has to be further analyzed using the cascade model.

In a cascade model, the polymer network is described by a branching tree where the junctions between two polymers are formed via a reaction between two functional groups (Dobson & Gordon, 1965). The number of elastically active network chains (EANC) per chain is thus determined by the functionalities and reaction equilibrium constant. The expression of the gel modulus can be assumed to be in the form of an ideal rubber, which is directly proportional to the number of EANC per chain. The cascade model

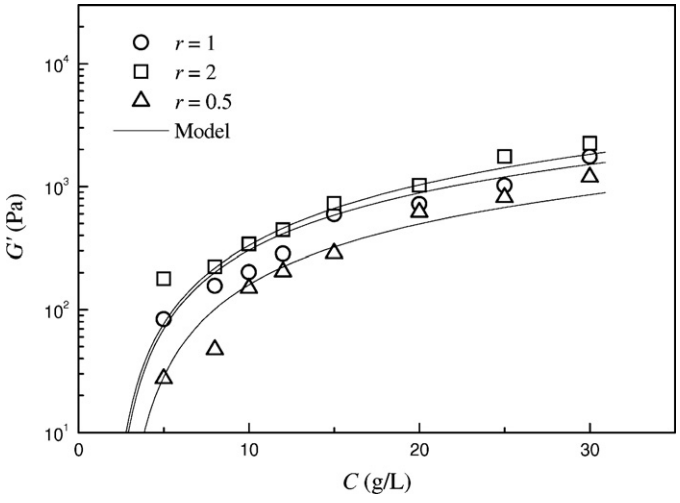


**Fig. 3.** Effect of concentration ratio on the concentration dependence of $G$ for KGM/XG mixed gels at 25 °C. The solid curves are derived by the cascade model using the parameters at the functionality set ($f_{KGM}$, $f_{XG}$) = (3, 100).

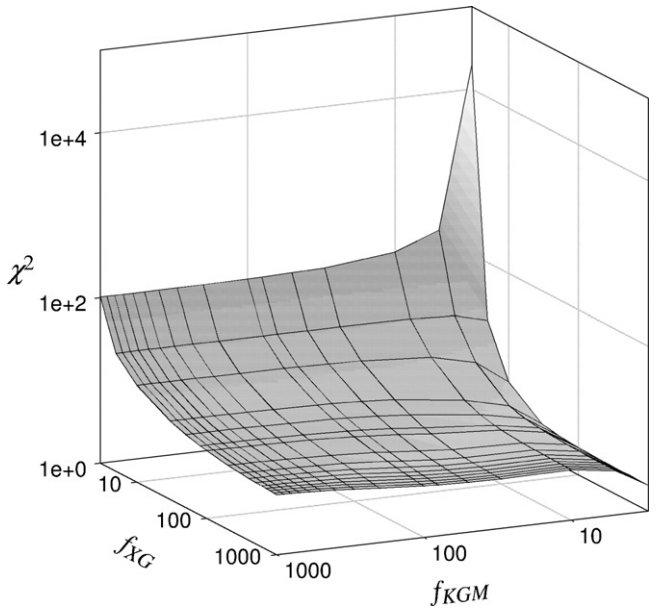


**Fig. 4.** The object function $\chi^2$ as a function of component functionalities obtained by fitting the modulus-concentration dependence data using Eq. (2).

developed for two-component synergistic gels (Mao, 2006; Mao & Chen, 2006) can be applied to the KGM/XG system by assuming a network formed via the interaction between KGM and XG. In the model formalism, the gel modulus for a KGM/XG mixed gel with concentrations, $C_{KGM}$ and $C_{XG}$, and molecular weights, $M_{KGM}$ and $M_{XG}$, has contributions from both components:

$$G = aRT\left[N_{eKGM}\left(\frac{C_{KGM}}{M_{KGM}}\right) + N_{eXG}\left(\frac{C_{XG}}{M_{XG}}\right)\right] \quad (1)$$

where $a$ is the front factor, which measures the deviation from ideal rubber behavior, and $N_{eKGM}$ and $N_{eXG}$ are the number of EANC per chain. $N_{eKGM}$ and $N_{eXG}$ are expressed as a function of the equilibrium constant $K$ and the functionalities $f_{KGM}$ and $f_{XG}$. The detail derivation of the model equation for a synergistic gel can be found elsewhere (Mao & Chen, 2006).

In order to estimate the cascade parameters, the modulus data at different mixing ratios were fitted numerically to the model by minimizing an object function $\chi^2$, which is defined as

$$\chi^2 = \sum(\ln G'^{\exp} - \ln G'^{cal})^2 \quad (2)$$

where $G'^{exp}$ and $G'^{cal}$ represent the experimental and calculated $G'$ values, respectively. The minimization process consists of a non-linear least-squares method using the Levenberg–Marquardt algorithm (Marquardt, 1963) to optimize the values of $a$ and $K$ and a direct search method to obtain the best-fit values of $f_{KGM}$ and $f_{XG}$. Fig. 4 shows the results of fitting the modulus data in Fig. 3 to the cascade model. The minimized object function $\chi^2$ is plotted as a function of $f_{KGM}$ and $f_{XG}$. It can be seen that the $\chi^2$ value varies smoothly with the functionalities and drops to a minimum in the low $f_{KGM}$ and high $f_{XG}$ region.

In Fig. 3, the minimum is located at ($f_{KGM}$, $f_{XG}$) = (3, 1000). A closer examination of the $\chi^2$ values near the minimum show that an increase in $f_{KGM}$ causes significant increase in $\chi^2$ value, whereas the $\chi^2$ value only changes slightly for $f_{XG}$ in the range 100–1000 at a fixed $f_{KGM}$ value of 3 (within 2% variation). Thus, the optimal $f_{KGM}$ value can be identified close to 3, while the possible $f_{XG}$ value may lie in the range of 100–1000. These values are consistent with our previous arguments that the $f_{KGM}$ and $f_{XG}$ values are quite different and the latter should be higher than the former. Furthermore, model curves derived using the cascade parameters at ($f_{KGM}$,

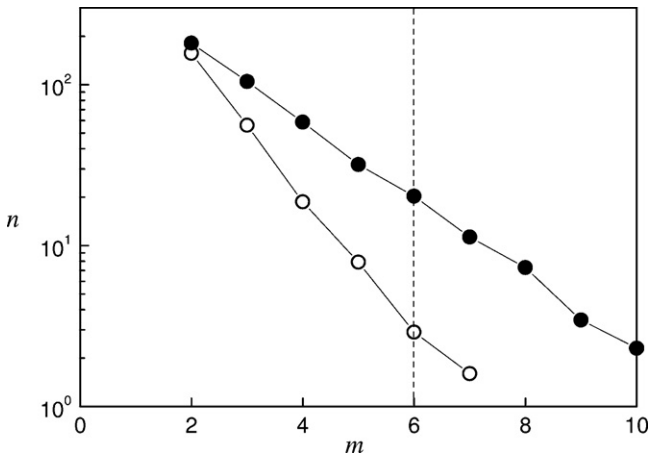


**Fig. 5.** Distribution of unsubstituted glucose (○) or mannose (●) segments in the konjac glucomannan chain ($m$: segment size; $n$: number of unsubstituted segments). The estimation was made based on a random distribution of glucose and mannose units along the polysaccharide backbone with a mannose/glucose ratio of 1.6. The content of acetyl groups was assumed to be one per 19 residues.

$f_{XG}$) = (3, 100) are plotted in Figs. 2 and 3, and in good agreement with the experimental data.

Now the physical significance of the optimal cascade parameters is discussed. First we examine the front factor $a$, which should have a value of unity if the gel elasticity results exclusively from the loss of conformational entropy of the network chains on deformation. In this case, the value of $a$ at ($f_{KGM}$, $f_{XG}$) = (3, 100–1000) is approximately 8.6, which is a typical value for physical gels, indicating the presence of an enthalpic contribution to the gel elasticity. For locust bean gum (LBG)/XG mixed gels, $a$ values of 5.4 and 3.0 have been reported (Mao & Rwei, 2006). When comparing these values, it seems that the network chain of KGM/XG gels is somewhat stiffer than that of LBG/XG gels.

Next, we check the values of the cascade parameters $f_{KGM}$ and $f_{XG}$, which can be related to the chemical structure of the corresponding polysaccharides. For konjac glucomannan, we have a value of $f_{KGM}$ = 3, implying that only a small fraction of the sugar residues in the glucomannan contributes to the interaction with xanthan. Now the question is which segment of the glucomannan corresponds to this extremely small functionality value. It has been demonstrated that for galactomannans, the interaction with xanthan is associated with the segment with more than six consecutive unsubstituted mannose residues (Dea et al., 1986). Since the konjac glucomannan contains both unsubstituted (without an acetyl group attached) mannose and glucose segments, it is likely that either one of them or both may bind with xanthan.

To answer this question, the distribution profile of unsubstituted mannose or glucose segments of different sizes for KGM was generated with a computer simulation by assuming a random distribution of mannose and glucose residues, along with acetyl groups, as shown in Fig. 5. If we calculate the number of segments with size greater than or equal to six units, it is found that the number of mannose segments is an order of magnitude higher than the optimal $f_{KGM}$ value, while the number of glucose segments is approximately four, which is consistent with the optimal $f_{KGM}$ value. This simulation suggests that the consecutive glucose segment with more than six units, rather than the mannose segment, is responsible for the interacting site for KGM/XG gels. A tentative scheme is given in Fig. 6 to illustrate the binding site of KGM/XG gels. A similar hypothesis was made by Goycoolea et al. (1995) based on the differences in thermal behavior between LBG/XG and KGM/XG gels. Here we provide strong evidence for the involvement of consecutive glucose residues in binding with xanthan.

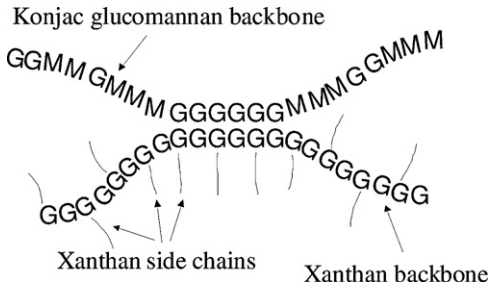


**Fig. 6.** The schematic representation of the binding of KGM to XG in KGM/XG mixed gels (G and M stand for mannose and glucose residues, respectively).

Although the cascade analysis shows that the appropriate $f_{XG}$ value ranges from 100 to 1000, the chemical structure of XG further imposes a limitation on the $f_{XG}$ value. The xanthan sample used here with a molecular weight of $0.98 \times 10^6$ g/mol consists of approximately 1090 repeating units (two glucose residues attached by a trisaccharide side chain), estimated by assuming a pyruvate content of 50% and an acetate content of 50%. It is reasonable to assume that the interacting site of xanthan involves at least three repeating units, which are comparable in length to six glucose residues in KGM. Thus, a physically consistent value of $f_{XG}$ should not exceed 360 in this case. By combining this consideration with the results of the cascade analysis, the appropriate $f_{XG}$ values can be narrowed down to the range of 100–360. At this point, the exact $f_{XG}$ value cannot be ascertained, and little can be said about the chemical nature of the binding site of xanthan.

### 3.2. Critical concentrations

Application of the cascade model to the critical condition of thermo-reversible gels can provide some useful information about the thermodynamics of the binding reaction. When heated above the melting point the gel loses its integrity due to a decrease in junction density, which is expressed as a function of polysaccharide concentration and mixing ratio. The relationship between the melting temperature and polysaccharide concentration at each mixing ratio can be fairly well described by the Eldridge–Ferry equation, as shown in Fig. 7. The slope of the fitted line is proportional to the enthalpy change of gel melting, which is relatively large at $r$ = 1 and 2. These data can be then used to construct the composition dependence of the critical concentration at different temperatures.

Fig. 8 shows the critical concentration $C_0$ of the KGM/XG mixed gel as a function of mixing ratio at different temperatures. It can

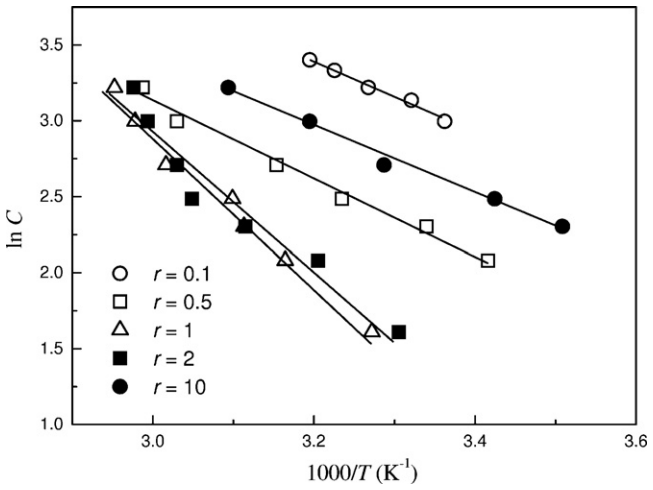


**Fig. 7.** Eldridge–Ferry plots for KGM/XG mixed gels at different mixing ratios.

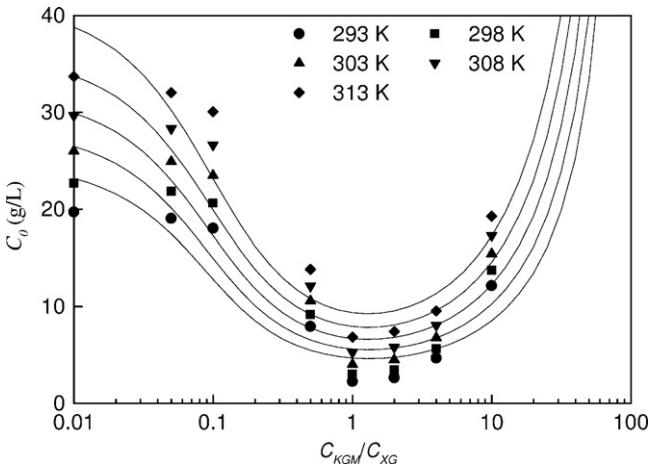


**Fig. 8.** Composition dependence of the critical concentration for KGM/XG mixed gels at different temperatures. The curves are derived by the cascade model using the parameters at the functionality set ($f_{KGM}$, $f_{XG}$) = (3, 20).

be seen that at a specific temperature, $C_0$ has a minimum as $C_{KGM}$ and $C_{XG}$ are comparable, and increases with increasing difference in mixing ratio. The $C_0$ curve tends to level off at high XG contents due to the homotypic association of xanthan. When increasing temperature, the critical concentration increases at all mixing ratios, demonstrating an increase in the breakup probability of gel junctions at elevated temperature.

The critical behavior in Fig. 8 can be described by a modified cascade model that we developed previously by including the effect of the homotypic association of one of the components (Mao, 2008). In the modified cascade model, the homotypic association of xanthan is assumed to occur at the same site as that responsible for the binding between KGM and XG. Then, the critical concentration can be obtained by calculating the critical conversion $\alpha_{XG0}$ for $f_{XG}$ in the following quadratic equation:

$$\frac{f_{XG}C_{XG}M_{KGM}x_0^2(f_{KGM}-1)}{f_{KGM}C_{KGM}M_{XG}}\alpha_{XG0}^2+(1-x_0)\alpha_{XG0}-\frac{1}{f_{XG}-1}=0 \qquad (3)$$

where $x_0$ is defined as the fraction of reacted $f_{XG}$ which binds with KGM at the gel point (when $x_0 = 1$, the homotypic association of xanthan is absent, and the above equation is reduced to the cascade model for synergistic mixed gels). To determine the critical conversion, both values of the equilibrium constants for the heterotypic and homotypic associations are required along with the functionalities $f_{EMG}$ and $f_{XG}$. The detailed relationship between $\alpha_{XG0}$ and the cascade parameters can be found elsewhere (Mao, 2008).

The parameters of the modified cascade model can be obtained by fitting the experimental data in Fig. 8 using Eq. (3). This is done by minimizing an object function $\chi^2$, which is defined as follows:

$$\chi^2=\sum(\ln C_0^{\exp}-\ln C_0^{cal})^2 \qquad (4)$$

where $C_0^{\exp}$ and $C_0^{cal}$ are the experimental and calculated $C_0$ values, respectively. The summation in Eq. (4) is taken over all the mixing ratios and temperatures investigated. The fitting result is shown in Fig. 9 by plotting $\chi^2$ as a function of $f_{KGM}$ and $f_{XG}$. It can be seen that the $\chi^2$ value does not vary smoothly with $f_{KGM}$ and $f_{XG}$, and there are many local minima of the object function. Nevertheless, the global minimum can be easily identify at ($f_{KGM}$, $f_{XG}$) = (3, 20), and the fitting curves derived by using this parameter set are in good agreement with the experimental data, as shown in Fig. 8.

The physical interpretation of the cascade parameters can be made in a manner similar to that in the previous section. The optimal $f_{KGM}$ value is identical to that obtained from the modulus data and points to the fact that consecutive glucose segments are

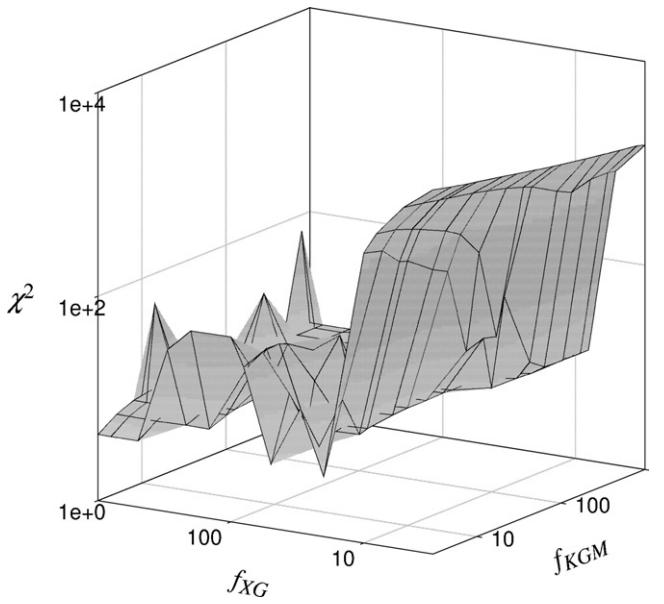


**Fig. 9.** The object function $\chi^2$ as a function of component functionalities obtained by fitting the critical concentration data using Eq. (4).

responsible for the interacting site for KGM/XG gels. The optimal $f_{XG}$ value, in contrast, is much lower than that obtained from the modulus data. The underestimation of the $f_{XG}$ value is possibly due to that the "test tube upside-down" method is a destructive method which measures the polysaccharide concentration required to support the gel against gravity. In this manner, the network junctions lost at elevated temperature as measured by the onset of flow should be fewer than those probed by the rheological method, thus leading to a low functionality value.

The temperature dependence of the equilibrium constants for the heterotypic association between KGM and XG and the homotypic association of XG can be further analyzed by the van't Hoff equation

$$K=\exp\left(\frac{\Delta S}{R}-\frac{\Delta H}{RT}\right) \qquad (5)$$

where $\Delta H$ and $\Delta S$ are the enthalpy change and entropy change per cross-link. Both types of association obey the van't Hoff relationship very well and the values of $\Delta H$ and $\Delta S$ can be readily calculated. Table 1 lists the calculated $-\Delta H$ and $-\Delta S$ values and compares them with those reported for LBG/XG gels (Mao, 2008). It can be seen that the $-\Delta H$ and $-\Delta S$ values of the homotypic association of xanthan are quite similar for both mixed gels, but, in contrast, the $-\Delta H$ and $-\Delta S$ values of the heterotypic association for the KGM/XG gel are surprisingly small as compared with those for the LBG/XG gel. This discrepancy suggests that KGM binds to xanthan in a different way. It is also of interest to note that for the KGM/XG gel, the enthalpy/entropy ratio for the heterotypic association is much higher than the value for the associations of low-molecular-weight

**Table 1**
Enthalpy changes, entropy changes, and enthalpy–entropy ratios for the bindings in KGM/XG gels and LBG/XG gels.

| Type of binding | $-\Delta H$ (kJ/mole) | $-\Delta S$ (J/(K mole)) | $\Delta H/300\Delta S$ |
|---|---|---|---|
| KGM/XG gels | | | |
| KGM–XG | 27 | 16 | 5.52 |
| XG–XG | 19 | 32 | 2.02 |
| LBG/XG gels | | | |
| LBG–XG | 81[a] | 173[a] | 1.56[a] |
| XG–XG | 23[a] | 33[a] | 2.28[a] |

[a] These values were taken from Mao (2008).

molecules in solution (1.59) (Searle, Westwell, & Williams, 1995). For the LBG/XG gel, the corresponding enthalpy entropy ratio is almost identical to the value of 1.59. This difference is mainly a consequence of the low entropy loss associated with the binding between KGM and XG.

A possible explanation of the low entropy loss for KGM/XG binding can be given below. The change in entropy for the binding process can be presented as a sum of two major contributions: (i) the entropy loss arising from a reduction in the availability of different configurations for the polysaccharides, and (ii) the hydrational entropy change due to the water molecules released to the bulk. The binding of XG backbone with the glucose units of KGM may result in significant dehydration of the interaction sites, thus producing a large hydrational entropy change, which partially compensates the configurational entropy loss of the polysaccharides. The gain in the hydrational entropy for LBG/XG gels, in contrast, is not significant due to the dissimilarity of the backbone sugar units and does not play an important role in the binding process, thus having a higher entropy loss and smaller enthalpy entropy ratio.

## 4. Conclusions

The concentration dependence of elastic moduli and the mixing-ratio dependence of critical concentration for KGM/XG gels were successfully described by the cascade model. The model assumes that the interaction between segments of KGM and XG reaches equilibrium and generates a cascade-type network. The fitting result shows that the best-fit front factor $a$ is greater than unity, which suggests the existence of an enthalpic contribution to the gel elasticity and is consistent with other polysaccharide gels. The optimal $f_{KGM}$ value is 3 for both fitting results. On the other hand, the possible $f_{XG}$ value obtained from the modulus data ranges from 100 to 1000, while that obtained from the critical data is 25. This discrepancy can be ascribed to that the gel networks probed by the "test tube upside-down" method are fewer than those probed by the rheological method.

The functionality values, in conjunction with the enthalpy/entropy ratio, were used to evaluate the possible interacting segment of the polysaccharides. We proposed that for konjac glucomannan, the interaction with XG takes place on the consecutive glucose residues of KGM with six or more units. The proposed binding site of KGM is supported by two findings: (i) an $f_{KGM}$ value of 3, which can only be assigned to the consecutive glucose residues, rather than mannose residues, and (ii) a high enthalpy/entropy ratio, which is attributed to the gain in the hydrational entropy due to the release of water molecules caused by the binding of the glucose units of KGM to the xanthan backbone. The major contribution of this work is to provide evidences for the interaction of KGM with XG taking place on the consecutive glucose residues of KGM, which explains the differences observed in the literature between KGM/XG and LBG/XG gels.

## Acknowledgment

This work was supported by the National Science Council of the Republic of China through the project NSC 97-2221-E-218-013.

## References

Agoub, A. A., Smith, A. M., Giannouli, P., Richardson, R. K., & Morris, E. R. (2007). "Melt-in-the-mouth" gels from mixtures of xanthan and konjac glucomannan under acidic conditions: A rheological and calorimetric study of the mechanism of synergistic gelation. *Carbohydrate Polymers*, *69*, 713–724.

Alvarez-Mancenido, F., Lacik, I., Landín, M., & Martínez-Pacheco, R. (2008). Konjac glucomannan and konjac glucomannan/xanthan gum mixtures as excipients for controlled drug delivery systems. Diffusion of small drugs. *International Journal of Pharmaceutics*, *349*, 11–18.

Berth, G., Dautzenberg, H., Christensen, B. E., Harding, S. E., Rother, G., & Smidsrød, O. (1996). Static light scattering studies on xanthan in aqueous solutions. *Macromolecules*, *29*, 3491–3498.

Brownsey, G. J., Cairns, P., Miles, M. J., & Morris, V. J. (1988). Evidence for intermolecular binding between xanthan and the glucomannan konjac mannan. *Carbohydrate Research*, *176*, 329–334.

Cairns, P., Miles, M. J., & Morris, V. J. (1986). Intermolecular binding of xanthan gum an carob gum. *Nature (London)*, *322*, 89–90.

Cairns, P., Miles, M. J., Morris, V. J., & Brownsey, G. J. (1987). X-ray fibre-diffraction studies of synergistic binary polysaccharide gels. *Carbohydrate Research*, *160*, 411–423.

Capron, I., Brigand, G., & Muller, G. (1997). About the native and renatured conformation of xanthan exopolysaccharide. *Polymer*, *38*, 5289–5295.

Clark, A. H., & Ross-Murphy, S. B. (1985). The concentration dependence of biopolymer gel modulus. *British Polymer Journal*, *17*, 164–168.

Dea, I. C. M., Clark, A. H., & McCleary, B. V. (1986). Effect of galactose-substitution-patterns on the interaction properties of galactomannans. *Carbohydrate Research*, *147*, 275–294.

Dea, I. C. M., Morris, E. R., Rees, D. A., Welsh, E. J., Barnes, H. A., & Price, J. (1977). Associations of like and unlike polysaccharides: Mechanism and specificity in galactomannans, interacting bacterial polysaccharides and related systems. *Carbohydrate Research*, *57*, 249–272.

Dobson, G. R., & Gordon, M. (1965). Theory of branching process and statistics of rubber elasticity. *The Journal of Chemical Physics*, *43*, 705–713.

Eldridge, J. E., & Ferry, J. D. (1954). Studies of the cross-linking process in gelatin gels. III. Dependence of melting point on concentration and molecular weight. *The Journal of Physical Chemistry*, *58*, 713–992.

Goycoolea, F. M., Richardson, R. K., Morris, E. R., & Gidley, M. J. (1995). Stoichiometry and conformation of xanthan in synergistic gelation with locust bean gum or konjac glucomannan: Evidence for heterotypic binding. *Macromolecules*, *28*, 8308–8320.

Hong, P. D., & Chen, J. H. (1998). Structure and properties of polyvinyl chloride physical gels. *Polymer*, *39*, 711–717.

Jansson, P. E., Kenne, L., & Lindberg, B. (1975). Structure of the extracellular polysaccharide from *Xanthomonas campestris*. *Carbohydrate Research*, *45*, 275–282.

Katsuraya, K., Okuyama, K., Hatanaka, K., Oshima, R., Sato, T., & Matsuzaki, K. (2003). Constitution of konjac glucomannan: Chemical analysis and $^{13}C$ NMR spectroscopy. *Carbohydrate Polymers*, *53*, 183–189.

Maeda, M., Shimahara, H., & Sugiyama, N. (1980). Detailed examination of the branched structure of konjac glucomannan. *Agricultural and Biological Chemistry*, *44*, 245–252.

Maekaji, K. (1974). The mechanism of gelation of konjac mannan. *Agricultural and Biological Chemistry*, *38*, 315–321.

Mao, C. F. (2006). Temperature dependence of gel properties of two-component physical gels. *Journal of Applied Polymer Science*, *102*, 663–673.

Mao, C. F. (2008). Self- and cross-associations in two-component mixed polymer gels. *Journal of Polymer Science Part B: Polymer Physics*, *46*, 80–91.

Mao, C. F., & Chen, J. C. (2006). Cascade model for coupled two-component polymer gels. *Journal of Applied Polymer Science*, *99*, 2771–2781.

Mao, C. F., & Rwei, S. P. (2006). Cascade analysis of mixed gels of xanthan and locust bean gum. *Polymer*, *47*, 7980–7987.

Marquardt, D. W. (1963). An algorithm for least-squares estimation of nonlinear parameters. *SIAM Journal on Applied Mathematics*, *11*, 431–441.

McCleary, B. V., Amado, R., Waibel, R., & Neukom, H. (1981). Effect of galactose content on the solution and interaction properties of guar and carob galactomannans. *Carbohydrate Research*, *92*, 269–285.

Melton, L. D., Mindt, L., Rees, D. A., & Sanderson, G. R. (1976). Covalent structure of the extracellular polysaccharide from *Xanthomonas campestris*: Evidence from partial hydrolysis studies. *Carbohydrate Research*, *46*, 245–257.

Milas, M., & Rinaudo, M. (1979). Conformational investigation on the bacterial polysaccharide xanthan. *Carbohydrate Research*, *76*, 189–196.

Milas, M., & Rinaudo, M. (1986). Properties of xanthan gum in aqueous solutions: Role of the conformational transition. *Carbohydrate Research*, *158*, 191–204.

Pai, V. B., & Khan, S. A. (2002). Gelation and rheology of xanthan/enzyme-modified guar blends. *Carbohydrate Polymers*, *49*, 207–216.

Prawitwong, P., Takigami, S., & Phillips, G. O. (2007). Effects of γ-irradiation on molar mass and properties of Konjac mannan. *Food Hydrocolloids*, *21*, 1362–1367.

Rodd, A. B., Dunstan, D. E., & Boger, D. V. (2000). Characterisation of xanthan gum solutions using dynamic light scattering and rheology. *Carbohydrate Polymer*, *42*, 159–174.

Ross-Murphy, S. B., Morris, V. J., & Morris, E. R. (1983). Molecular viscoelasticity of xanthan polysaccharide. *Faraday Symposia of the Chemical Society*, *18*, 115–129.

Searle, M. S., Westwell, M. S., & Williams, D. H. (1995). Application of a generalised enthalpy–entropy relationship to binding co-operativity and weak associations in solution. *Journal of the Chemical Society Perkin Transactions*, *2*, 141–151.

Smith, I. H., Symes, K. C., Lawson, C. J., & Morris, E. R. (1981). Influence of the pyruvate content of xanthan on macromolecular association in solution. *International Journal of Biological Macromolecules*, *3*, 129–134.